AGU PUBLICATIONS

Geophysical Research Letters

RESEARCH LETTER
10.1002/2016GL070898

Key Points:
- Model MJO amplitude is found to be closely tied to a model's convective moisture adjustment time scale
- Strength of surface flux and radiative heating is found to be negatively correlated to MJO amplitude across multimodel simulations
- Models with a shorter convective time scale is characterized by weaker and more bottom-heavy vertical velocity profile

Supporting Information:
- Supporting Information S1

Correspondence to:
X. Jiang,
xianan@ucla.edu

Citation:
Jiang, X., M. Zhao, E. D. Maloney, and D. E. Waliser (2016), Convective moisture adjustment time scale as a key factor in regulating model amplitude of the Madden-Julian Oscillation, *Geophys. Res. Lett.*, *43*, doi:10.1002/2016GL070898.

Received 18 AUG 2016
Accepted 25 SEP 2016
Accepted article online 27 SEP 2016

Convective moisture adjustment time scale as a key factor in regulating model amplitude of the Madden-Julian Oscillation

Xianan Jiang[1,2], Ming Zhao[3], Eric D. Maloney[4], and Duane E. Waliser[2]

[1]Joint Institute for Regional Earth System Science and Engineering, University of California, Los Angeles, California, USA, [2]Jet Propulsion Laboratory, California Institute of Technology, Pasadena, California, USA, [3]Geophysical Fluid Dynamics Laboratory/NOAA, Princeton University, Princeton, New Jersey, USA, [4]Department of Atmospheric Science, Colorado State University, Fort Collins, Colorado, USA

Abstract Despite its pronounced impacts on weather extremes worldwide, the Madden-Julian Oscillation (MJO) remains poorly represented in climate models. Here we present findings that point to some necessary ingredients to produce a strong MJO amplitude in a large set of model simulations from a recent model intercomparison project. While surface flux and radiative heating anomalies are considered important for amplifying the MJO, their strength per unit MJO precipitation anomaly is found to be negatively correlated to MJO amplitude across these multimodel simulations. However, model MJO amplitude is found to be closely tied to a model's convective moisture adjustment time scale, a measure of how rapidly precipitation must increase to remove excess column water vapor, or alternately the efficiency of surface precipitation generation per unit column water vapor anomaly. These findings provide critical insights into key model processes for the MJO and pinpoint a direction for improved model representation of the MJO.

1. Introduction

The tropical atmosphere exhibits pronounced intraseasonal fluctuations. The Madden-Julian Oscillation (MJO), named after its two discoverers [*Madden and Julian,* 1971, 1972], is the most prominent tropical intraseasonal variability mode and is characterized by a planetary-scale circulation that is strongly coupled to deep convection and slow eastward migration along the equator at about 5° of longitude per day. While the most vigorous convective signal of the MJO is observed over the Indo-Pacific region, widespread influences of the MJO on weather extremes worldwide, e.g., hurricanes, floods, wild fires, and air quality, have been extensively reported [*Maloney and Hartmann*, 2000; *Zhang*, 2013]. The predictability of the quasiperiodic MJO [*Waliser*, 2012; *Neena et al.,* 2014] provides an important avenue for extended-range prediction of these extreme weather events not only in the tropics but also the extratropics [e.g., *Cassou*, 2008; *L'Heureux and Higgins*, 2008; *Lin et al.,* 2009]. Further, the intraseasonal changes in atmospheric conditions associated with the MJO can significantly impact lower frequency variability (e.g., El Niño–Southern Oscillation) and the climate state of the global atmosphere-ocean system [e.g., *McPhaden*, 1999; *Kessler and Kleeman*, 2000; *Grise and Thompson*, 2011].

While the MJO's pivotal role in the global climate system and in weather and seasonal-to-subseasonal (S2S) prediction has been fully recognized [*Vitart et al.,* 2012; *Zhang et al.,* 2013; *National Academy of Sciences*, 2016], the capability of current global climate models to simulate the MJO remains rather limited, including large model biases in simulating both the MJO amplitude and its eastward propagation [*Hung et al.,* 2013; *Jiang et al.,* 2015]. Along with impeding the skill of weather and S2S forecasts, these model deficiencies also leave us greatly disadvantaged in conducting future climate projections, particularly in projections of extreme events that are significantly modulated by the MJO. In this study, with an eye toward identifying the elusive model ingredients needed for improving MJO simulations in weather forecasting and climate models, we present results that highlight a critical process that appears to regulate model MJO amplitude in climate models that participated in a recent multimodel MJO comparison project.

2. Data and Approach

2.1. Multimodel Climate Simulation and Observational Data Sets

Simulations from 25 climate models analyzed in this study are from the recent MJO Task Force and Global Energy and Water cycle Exchanges Global Atmospheric System Studies MJO model comparison project

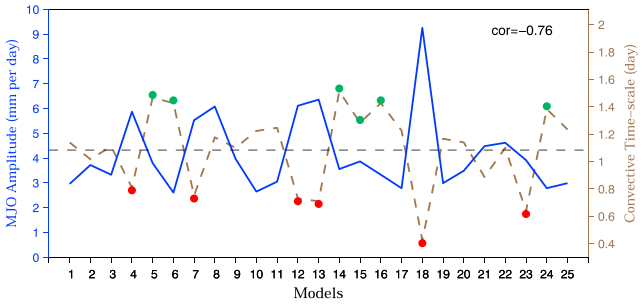

Figure 1. MJO amplitude and model convective moisture adjustment time scale. The MJO amplitude (blue curves) in each model is defined by the standard deviation of 20–100 day band-pass filtered rainfall over the Indian Ocean (75–85°E; 10°S–10°N) during boreal winter (November–April; see supporting information Figure S1 for maps of MJO amplitude over the entire Indo-Pacific region). Following previous studies, convective time scale in each model is defined by the ratio of precipitable water (*W*) anomaly to precipitation (*P*) anomaly associated with the MJO and derived by a regression approach. Before conducting the regression, both *W* and *P* anomalies are subject to 20–100 day filtering and averaged over the Indian Ocean (75–85°E; 10°S–10°N) box. The horizontal dashed line denotes MJO amplitude and convective time scale in observations. Red (green) dots denote models with longer (shorter) convective time scales and will be used for later composite analyses. Model details corresponding to each model number in *x* axis can be found in the supporting information Table S1.

[*Petch et al.,* 2011; *Jiang et al.,* 2015; *Klingaman et al.,* 2015]. Each participating model was integrated for 20 years, either with an atmospheric-only general circulation model (AGCM) or an atmosphere-ocean coupled system. A list of participating models with their horizontal and vertical resolutions is provided in Table S1 in the supporting information. Output from all the participating GCMs was archived every 6 h on $2.5° \times 2.5°$ horizontal grids and 22 vertical pressure levels. Daily averaged data are used for this study.

The primary observational data sets used for this study include Tropical Rainfall Measuring Mission-based rainfall observations (version 3B42 v7) [*Huffman et al.,* 1995] and the European Center for Medium range Weather Forecasting ERA-Interim reanalysis [*Dee et al.,* 2011] for the period of 1998–2012.

2.2. Moist Entropy and Gross Moist Stability

In this study, the MJO instability is examined by analyzing the moist static energy processes under a "moist mode" framework for the MJO [*Yu and Neelin*, 1994; *Raymond*, 2001; *Sobel and Maloney*, 2013]. Specifically, we employ moist entropy equation instead of conventional moist static energy equation following *Raymond et al.* [2009] and *Benedict et al.* [2014], namely,

$$T_R[\partial s/\partial t] = -T_R\left[\overrightarrow{v}\cdot\nabla s\right] - T_R[\omega(\partial s/\partial p)] + F_s + R \quad (1)$$

where the square brackets represent a mass-weighted vertical integral from 1000 hPa to 100 hPa, *s* is the specific moist entropy, T_R is the reference temperature of 273.15 K, $\overrightarrow{v}$ is the horizontal vector winds, ω the vertical pressure velocity, F_s is total surface fluxes including sensible and latent heat fluxes, and *R* is vertically integrated radiative (short wave and long wave) heating. Correspondingly, the gross moist stability can be derived by horizontal and vertical moist entropy transport per unit MJO precipitation.

2.3. Analysis Methods

Intraseasonal variability signals in rainfall were extracted by applying a Lanczos bandpass time filter [*Duchon*, 1979] to retain variability with a period between 20 and 100 days. MJO amplitude is then defined by the standard deviations of winter intraseasonal rainfall (Figure S1). In this study, we focus our analyses over the Indian Ocean. Various fields associated with active MJO convection over the Indian Ocean are derived by simultaneous regressions of these daily fields onto the band-pass filtered rainfall averaged over the box region of 75–85°E; 5°S–5°N and scaled by 3 mm d^{-1} of rainfall at the base point for both observations and model simulations. Examination of the moist entropy budget was then performed over the MJO center 75–85°E; 5°S–5°N. Note that while MJO amplitude in each model simulation is sampled over the equatorial Indian Ocean, in general, it represents well the model MJO amplitude over the entire Indo-Pacific region (see supporting information Figures S1 and S2).

3. Results

Model simulated MJO amplitude over the Indian Ocean exhibits substantial intermodel variability, ranging from about 2.5 to 9.5 mm d^{-1}, versus 4.2 mm d^{-1} in the observations (Figure 1; left axis/blue line). Theoretical interpretation of MJO amplification is ascribed to feedback processes responsible for growth of

an initial convection perturbation. A recent school of thought that regards the MJO as a "moisture mode" provides a convenient framework for understanding essential physics of the MJO [*Yu and Neelin*, 1994; *Raymond*, 2001; *Sobel and Maloney*, 2013; *Pritchard and Bretherton*, 2014; *Adames and Kim*, 2016]. Under this framework, MJO precipitation (P) is primarily controlled by processes regulating precipitable water (W; i.e., atmospheric column water vapor), variations of which are equivalent to variations in column moist static energy under the weak-temperature-gradient conditions applicable over the Indo-Pacific region where the MJO convection is most active [*Raymond*, 2001; *Sobel et al.,* 2001]. The great sensitivity of P to W in tropics, which is a key tenet of moisture mode theory, is supported by observations [*Bretherton et al.,* 2004; *Peters and Neelin*, 2006; *Holloway and Neelin*, 2009]. In particular, *Bretherton et al.* [2004] identified a universal quasi-exponential relationship over all tropical oceans between P and column relative humidity r, defined by the ratio of W to its corresponding saturation water vapor path (W_s), which is also evident in model studies [*Raymond et al.,* 2007].

By examining instability of the moist entropy equation (equation (1)), two processes were previously identified as energy sources for the MJO, namely, anomalous column radiative heating (R) and surface heat fluxes (F_s). Anomalous radiative heating is mainly produced by reducing long-wave cooling through enhanced cloudiness and water vapor over the MJO convectively active region [*Raymond*, 2001; *Andersen and Kuang*, 2012], while the latter is mainly due to enhanced wind-driven surface latent heat fluxes [*Sobel et al.,* 2008; *Maloney et al.,* 2010]. Interaction between these two processes and convection thus serves as two positive feedback processes in amplifying MJO convection. The strengths of these feedbacks have traditionally been represented by the magnitudes of R and F_s per unit MJO precipitation. The stronger these two positive feedbacks are, the stronger MJO will be in a numeric model [*Raymond*, 2001; *Sobel and Maloney*, 2013]. On the other hand, overturning circulations induced by atmospheric heating associated with MJO convection acts to remove moist energy from active convection regions, serving as a negative feedback for MJO energetics. The net moist energy export by the circulation per unit MJO precipitation, or gross moist stability (GMS) [*Raymond et al.,* 2009; *Benedict et al.,* 2014; *Maloney et al.,* 2014], is often used to measure the strength of this negative convection-circulation feedback for the MJO. Previous study indicates that smaller positive values of the GMS correspond to stronger MJO amplitude [*Benedict et al.,* 2014; *Maloney et al.,* 2014]. We note that radiative heating anomalies are responsible for driving a portion of the circulation anomaly during MJO convective periods, and so the effects of radiative heating cannot be completely disentangled from those of convective heating in our definition of GMS.

Analysis based on multimodel simulations suggests that the model MJO amplitude indeed shows negative correlations to both horizontal and vertical components of GMS over the MJO convection region (Figures 2a and 2b). In particular, a marked negative correlation between the model MJO amplitude and total GMS is noted with a coefficient of −0.68 (Figure 2c), affirming the aforementioned negative convection-circulation feedback for the MJO. However, significant negative correlations are also evident between model MJO amplitude and strength of F_s and R, with correlations of −0.77 and −0.65 for F_s and R, respectively (Figures 2d and 2e). An even higher magnitude of correlation (−0.82) is evident when the MJO amplitude is correlated to sum of these two energy input terms, suggesting that some other process determines the spread in MJO amplitude among the models.

Since R and F_s are largely balanced by energy exports through the overturning circulation, the fact that model MJO amplitude is negatively correlated to both moist energy source and sink terms motivated us to further explore the association between the model MJO amplitude and strength of MJO moist energy per unit precipitation across model simulations. In agreement with the weak-temperature-gradient theory, column moist energy variations are dominated by precipitable water W (figure not shown). Column moist energy anomalies per unit precipitation anomaly, therefore, can be effectively represented by W anomaly per unit P anomaly, which is equivalent to the convective moisture adjustment time scale (τ_c) proposed in several previous studies [*Yu and Neelin*, 1994; *Bretherton et al.,* 2004; *Sobel and Maloney*, 2012]. Physically, τ_c is the adjustment time for convection to respond to a departure from the "quasi-equilibrium" state in the atmospheric moisture field. Significant multimodel variations in τ_c, derived by corresponding anomalous W per unit P associated with the MJO using a regression approach, is clearly evident in Figure 1 with a range from 0.5 to 2 days (Figure 1). Note that a τ_c of about 1.1 days can be derived from observations with the same approach, in contrast to a τ_c of 2.4 days previously used in an idealized MJO model by *Sobel and Maloney* [2012] and a τ_c of about 0.6 days by *Adames and Kim* [2016]. Particularly noteworthy is the striking anticorrelation between

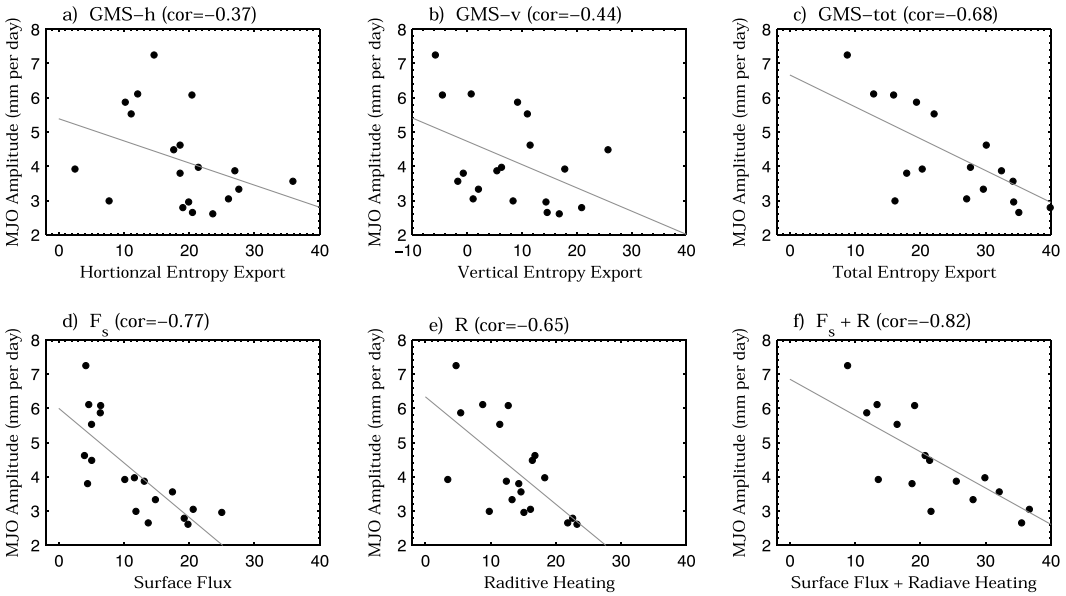

Figure 2. Scatterplots of strengths of moist energy exports, surface fluxes, and radiative forcing per unit precipitation and the MJO amplitude across multimodel simulations. The MJO amplitude on *y* axis in each panel is defined in the same way as in Figure 1. Variable on *x* axis in each panel denotes vertical (1000–100 hPa) integrals of (a) horizontal, (b) vertical, and (c) total moist energy export, (d) surface energy flux input F_s, (e) radiative heating *R*, (f) and $F_s + R$, respectively, averaged over the MJO convection center (75–85°E; 10°S–10°N). All these perturbation fields associated with the MJO are derived by regressions onto 20–100 day filtered rainfall over the Indian Ocean box (75–85°E; 10°S–10°N) and scaled by 3 mm d^{-1} of rainfall anomaly at the base point in all models.

model MJO amplitude and τ_c across these simulations, with a value of −0.76. Models that simulate stronger (weaker) MJO amplitude are characterized by shorter (longer) τ_c. Or in other words, models with stronger (weaker) MJO exhibit more (less) efficiency in producing surface precipitation per unit *W*. Noteworthy is that the τ_c associated with the MJO as shown in Figure 1 based on intraseasonal filtered daily *W* and *P* anomalies exhibits pronounced correlations (0.93) with the τ_c derived by unfiltered daily *W* and *P* values, with the unfiltered τ_c about half of values of intraseasonal τ_c (supporting information Figure S3). This result lends confidence to robustness of convective time scale as an intrinsic model characteristic rather than a spurious feature due to temporal filtering.

The relationship between *W* and *P* anomalies in model simulations is further examined by conducting composites of *W* anomaly as a function of *P* anomaly on model grids over the Indian Ocean. Derived *W* versus *P* profiles in different models are further averaged for three model groups, namely, with shorter τ_c, longer τ_c (denoted by red and green dots in Figure 1), and intermediate τ_c (remaining models except those denoted by red or green dots), and are illustrated by red, green, and black curves in Figure 3a, respectively. While difference in slope of *W* - *P* profiles is readily seen, the composite *W* - *P* profiles for all these three model groups illustrate a largely linear relationship between *W* and *P*, justifying a constant τ_c used for parameterizing *P* using *W* in previous theoretical MJO studies [*Sobel and Maloney*, 2012; *Adames and Kim*, 2016].

To further understand key processes responsible for different τ_c in climate models, we analyze the previously observed universal quasi-exponential *r* - *P* relationship [*Bretherton et al.*, 2004], i.e.,

$$P(r) = P_R \ \exp(a_d r) \tag{2}$$

where *r* is column relative humidity, $a_d = 15.6$, and $P_R = 8.22 \times 10^{-5}$ mm d^{-1}. By defining τ_c associated with the MJO, i.e., $\tau_c = \delta W/\delta P$, where δ denotes a small perturbation on intraseasonal time scale relative to a quasi-equilibrium state, we can obtain the following approximation for τ_c following *Sobel and Maloney* [2012]:

$$\tau_c \cong \overline{W}_s/(a_d P_0) \tag{3}$$

where $\overline{W}_s$ is seasonal mean saturated water vapor path, $a_d = \delta(lnP)/\delta r$ based on equation (2), depicting the rapidness of precipitation in responding to column moisture, and $P_0 = \delta P/\delta lnP$, defined as the reference

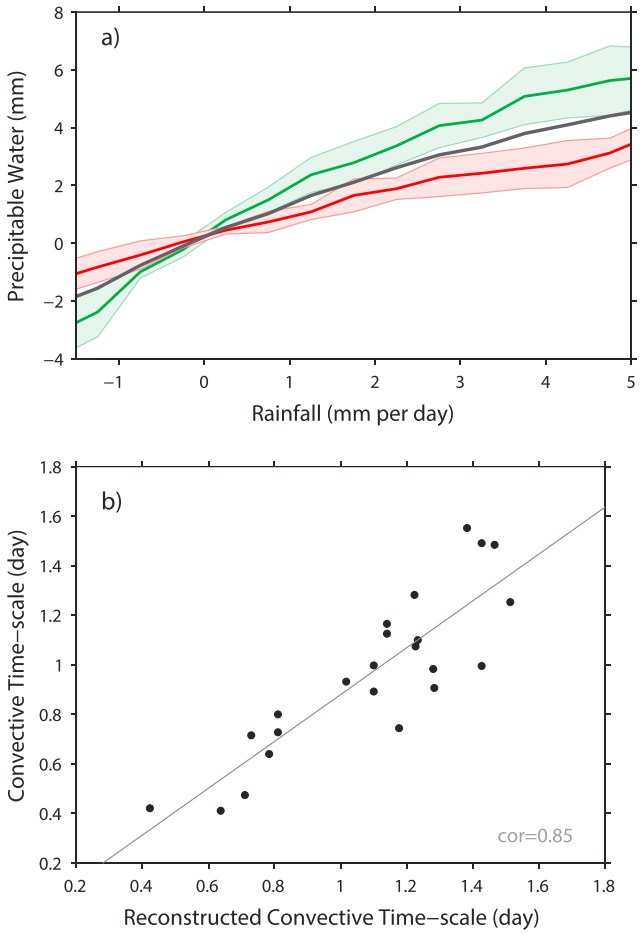

Figure 3. Precipitable water and precipitation relationship associated with the MJO in models with different convective moisture adjustment time scales. (a) Composite precipitable water perturbations averaged over precipitation bins for model grids over the Indian Ocean during boreal winter (November–April) in models with shorter (red), longer (green), and intermediate (black) convective time scales; (b) scatterplot of convective time scales directly calculated by ($\delta W/\delta P$) *y* axis and those reconstructed based on equation (3) (*x* axis).

background precipitation. In order to derive equation (3) and apply it to model simulations, several approximations are necessary, including the assumptions of negligible variations of W_s on the MJO time scale, the validity of r-P relationship as depicted in equation (1) for the model atmospheres, and small amplitude in δP compared to P_0. Practically, a_d and P_0 can be calculated by the regression approach with intraseasonal perturbations of lnP, P, and r. Reconstructed τ_c can then be derived for each model with corresponding $\overline{W}_s$, a_d, and P_0 based on equation (3). A high correlation (0.85) between directly derived τ_c by its definition ($\delta W/\delta P$) and reconstructed τ_c is evident (Figure 3b), suggesting that the equation (3) provides an excellent estimate of τ_c. Also note that reconstructed τ_c exhibits lower values than the directly derived τ_c in several models, largely due to biases in estimating P_0 by $\delta P/\delta lnP$ due to nonlinear fitting between δP and δlnP in these model simulations (figure not shown). Based on reconstructed τ_c, key factors responsible for differences in model τ_c can be further indicated by correlating τ_c to $\overline{W}_s$, a_d, and P_0, respectively. Correlation coefficients of −0.05, −0.41, and −0.6 are noted between τ_c and $\overline{W}_s$, a_d, and P_0, respectively. Therefore, both model variations in a_d and P_0, while not $\overline{W}_s$, are responsible for different τ_c across model simulations, suggesting realistic representation of the r-P relationship (rapidness of precipitation in responding to column moisture) and background precipitation are essential to get realistic τ_c in climate models.

To further gain insights into model processes associated with different τ_c, vertical structures of various dynamical and thermodynamical fields associated with MJO convection in models with longer and shorter τ_c are further examined by conducting composites over the two model groups. Shown in Figure 4, for the same amount of MJO precipitation (3 mm d^{-1}) over the Indian Ocean, the models with a shorter τ_c are characterized by weaker overturning circulations and atmospheric diabatic heating, along with lower cloud fractions and lower tropospheric moisture. These results are in accord with a more efficient precipitation-generating regime in the models with a shorter τ_c. Also noteworthy are the more vertically bottom-heavy profiles in the upward motion (Figure 4c) and heating (Figure 4f), if defined by a ratio of their values between the middle-upper (300–500 hPa) and lower (600–850 hPa) troposphere, in models with a shorter τ_c. More bottom-heavy upward motion feeds convection more effectively through upward moisture advection because of the stronger vertical moisture gradient in the lower troposphere. It also reduces net export of column moist energy, thus leading to stronger MJO instability, in concert with the stronger MJO (or shorter τ_c) models having lower GMS (Figure 2c), as has been documented in previous studies [e.g., *Maloney et al.*, 2014;

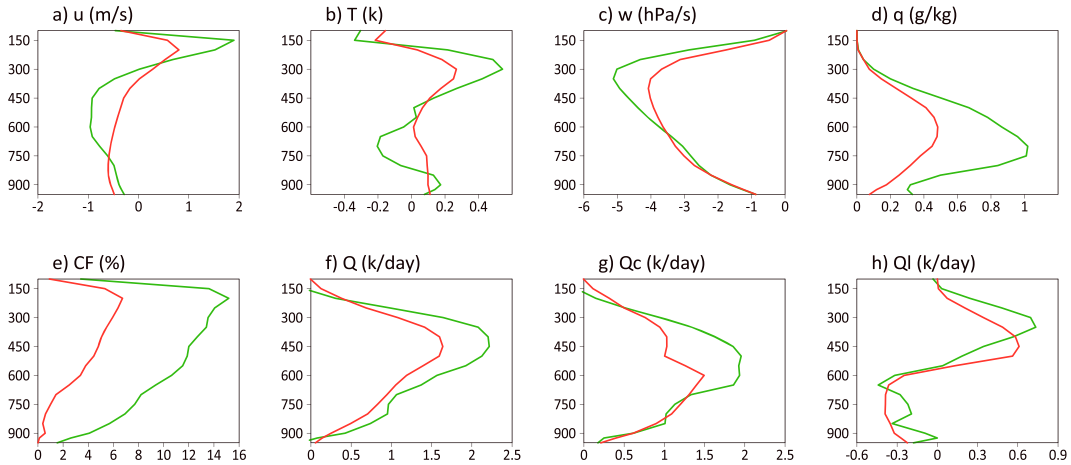

Figure 4. Vertical structures associated with MJO convection over the eastern equatorial Indian Ocean in models with shorter (red) and longer (green) τ_c: (a) *u* wind, (b) temperature, (c) *p* level vertical velocity, (d) specific humidity, (e) cloud fractions, (f) total latent heat, (g) convective heating, and (h) large-scale condensation. Vertical profiles of all these fields are derived by regressions onto 20–100 day filtered rainfall over the equatorial Indian Ocean (75–85°E;5°S–5°N) during boreal winter (November–April) and averaged over the MJO convective center except for *u* wind which was averaged over the equatorial region to the east of convection (85–120°E; 5°S–5°N). Definition for models with longer and shorter τ_c follows Figure 1.

Peters and Bretherton, 2006]. A decomposition of total atmospheric heating into convective and grid-scale components illustrates that the more bottom-heaviness structure in models with shorter τ_c is mainly due to the convective heating (Figures 4g and 4h, note different scales on *x* axes), suggesting that a different τ_c and associated vertical MJO structures across multimodel simulations could be largely due to processes in model cumulus parameterization. Recent studies confirm that model uncertainties in describing convective precipitation formation from cumulus condensate can lead to significant spread in the model climatology, including vertical structures of clouds and associated updrafts and radiative feedbacks, and lead to drastically different climate sensitivity [*Zhao*, 2014; *Zhao et al.,* 2016].

While our results suggest a close link between the model rainfall efficiency and convective time scale, the detailed model physics responsible for different τ_c in the 25 models examined here, however, remains unclear due to lack of more detailed model output. For example, an increase of model entrainment rate tends to produce a more bottom-heavy MJO structure [*Hannah and Maloney*, 2011], leading to improvement of MJO simulations in both amplitude and propagation. While the τ_c defined here is different from the convective adjustment time scale used in several model parameterization schemes [e.g., *Zhang and Mcfarlane*, 1995], which characterizes the time scale with which convective available potential energy is removed at an exponential rate by convection, improvement of MJO simulation was also noted by shortening the adjustment time scale in parameterizing cumulus convection [*Boyle et al.,* 2015].

4. Summary

Motivated by a longstanding and urgent need to improve the MJO in current weather forecasting and climate models, we identify a critical characteristic of modeled deep convection responsible for the MJO amplitude based on multimodel simulations from a recent international model comparison project. While surface flux and radiative heating anomalies are considered important for destabilizing the MJO, their strengths per unit MJO precipitation anomaly are each found to be negatively correlated to MJO amplitude across model simulations. A particularly interesting finding from this study is the striking out-of-phase relationship between the model MJO amplitude and the convective adjustment time scale. Models with stronger (weaker) MJO amplitude are generally characterized by a shorter (longer) convective time scale (τ_c). We further illustrate that different τ_c in these models is largely attributed to model differences in depicting the *r* - *P* relationship and amplitude of background precipitation. Moreover, models with a shorter τ_c tend to be more efficient at producing precipitation, with weaker upward motion and less cloud fraction per unit MJO precipitation

compared to models with longer τ_c. More bottom-heavy profiles in vertical motion and diabatic heating associated with MJO convection are also discerned in models with a shorter τ_c, mainly due to parameterized convective processes. While key model parameters responsible for different model τ_c remain an interesting open question and warrant further investigation, this study provides critical insights into key model processes for MJO physics and pinpoints a direction for improved model MJO representation in current climate models. Moreover, the convective time scale in a model can also be an excellent diagnostic metric for weather forecasting and climate model assessment purposes.

Acknowledgments

The multimodel output collected by this project and analyzed in this study is available for free download from https://earthsystemcog.org/projects/gassyotc-mip. X. Jiang acknowledges support by National Science Foundation (NSF) Climate and Large-Scale Dynamics Program under awards AGS-1228302 and NOAA Climate Program Office (CPO) under award NA12OAR4310075, NA15OAR4310098, and NA15OAR4310177. D. Waliser acknowledges the Office of Naval Research under project ONRBAA12-001, NSF award AGS-1221013, NASA Modeling, Analysis and Prediction Program, and the Jet Propulsion Laboratory, California Institute of Technology, under a contract with the NASA. E. Maloney acknowledges support by the NOAA MAPP program under awards NA13OAR431016, NA15OAR4310099, and NA15OAR4310098 and by NSF award AGS-1441916.

References

Adames, Á. F., and D. Kim (2016), The MJO as a dispersive, convectively coupled moisture wave: Theory and observations, *J. Atmos. Sci.*, *73*, 913–941, doi:10.1175/JAS-D-15-0170.1.

Andersen, J. A., and Z. Kuang (2012), Moist static energy budget of MJO-like disturbances in the atmosphere of a zonally symmetric aquaplanet, *J. Climate*, *25*, 2782–2804, doi:10.1175/jcli-d-11-00168.1.

Benedict, J. J., E. D. Maloney, A. H. Sobel, and D. M. W. Frierson (2014), Gross moist stability and MJO simulation skill in three full-physics GCMs, *J. Atmos. Sci.*, *71*, 3327–3349, doi:10.1175/JAS-D-13-0240.1.

Boyle, J. S., S. A. Klein, D. D. Lucas, H. Y. Ma, J. Tannahill, and S. Xie (2015), The parametric sensitivity of CAM5's MJO, *J. Geophys. Res. Atmos.*, *120*, 1424–1444, doi:10.1002/2014JD022507.

Bretherton, C. S., M. E. Peters, and L. E. Back (2004), Relationships between water vapor path and precipitation over the tropical oceans, *J. Climate*, *17*, 1517–1528.

Cassou, C. (2008), Intraseasonal interaction between the Madden-Julian Oscillation and the North Atlantic Oscillation, *Nature*, *455*, 523–527.

Dee, D. P., et al. (2011), The ERA-Interim reanalysis: configuration and performance of the data assimilation system, *Quart. J. Roy. Meteor. Soc.*, *137*, 553–597, doi:10.1002/qj.828.

Duchon, C. E. (1979), Lanczos filtering in one and two dimensions, *J. Appl. Meteorol.*, *18*, 1016–1022.

Grise, K. M., and D. W. J. Thompson (2011), Equatorial planetary waves and their signature in atmospheric variability, *J. Atmos. Sci.*, *69*, 857–874, doi:10.1175/jas-d-11-0123.1.

Hannah, W. M., and E. D. Maloney (2011), The role of moisture–convection feedbacks in simulating the Madden–Julian Oscillation, *J. Climate*, *24*, 2754–2770, doi:10.1175/2011jcli3803.1.

Holloway, C. E., and J. D. Neelin (2009), Moisture vertical structure, column water vapor, and tropical deep convection, *J. Atmos. Sci.*, *66*, 1665–1683, doi:10.1175/2008jas2806.1.

Huffman, G. J., R. F. Adler, B. Rudolf, U. Schneider, and P. R. Keehn (1995), Global precipitation estimates based on a technique for combining satellite-based estimates, rain-gauge analysis, and NWP model precipitation information, *J. Climate*, *8*, 1284–1295.

Hung, M.-P., J.-L. Lin, W. Wang, D. Kim, T. Shinoda, and S. J. Weaver (2013), MJO and convectively coupled equatorial waves simulated by CMIP5 climate models, *J. Climate*, *26*, 6185–6214, doi:10.1175/JCLI-D-12-00541.1.

Jiang, X., et al. (2015), Vertical structure and physical processes of the Madden-Julian oscillation: Exploring key model physics in climate simulations, *J. Geophys. Res. Atmos.*, *120*, 4718–4748, doi:10.1002/2014JD022375.

Kessler, W. S., and R. Kleeman (2000), Rectification of the Madden-Julian Oscillation into the ENSO cycle, *J. Climate*, *13*, 3560–3575.

Klingaman, N. P., X. Jiang, P. K. Xavier, J. Petch, D. Waliser, and S. J. Woolnough (2015), Vertical structure and physical processes of the Madden-Julian oscillation: Synthesis and summary, *J. Geophys. Res. Atmos.*, *120*, 4671–4689, doi:10.1002/2015JD023196.

L'Heureux, M. L., and R. W. Higgins (2008), Boreal winter links between the Madden-Julian Oscillation and the Arctic Oscillation, *J. Climate*, *21*, 3040–3050, doi:10.1175/2007jcli1955.1.

Lin, H., G. Brunet, and J. Derome (2009), An observed connection between the North Atlantic Oscillation and the Madden-Julian Oscillation, *J. Climate*, *22*, 364–380, doi:10.1175/2008jcli2515.1.

Madden, R. A., and P. R. Julian (1971), Detection of a 40–50 day oscillation in zonal wind in tropical Pacific, *J. Atmos. Sci.*, *28*, 702–708.

Madden, R. A., and P. R. Julian (1972), Description of global-scale circulation cells in tropics with a 40–50 day period, *J. Atmos. Sci.*, *29*, 1109–1123.

Maloney, E., X. Jiang, S.-P. Xie, and J. Benedict (2014), Process-oriented diagnosis of East Pacific warm pool intraseasonal variability, *J. Climate*, *27*, 6305–6324.

Maloney, E. D., and D. L. Hartmann (2000), Modulation of Eastern North Pacific Hurricanes by the Madden-Julian Oscillation, *J. Climate*, *13*, 1451–1460.

Maloney, E. D., A. H. Sobel, and W. M. Hannah (2010), Intraseasonal variability in an aquaplanet general circulation model, *J. Adv. Model. Earth Syst.*, *2*, doi:10.3894/james.2010.2.5.

McPhaden, M. J. (1999), Genesis and evolution of the 1997–98 El Nino, *Science*, *283*, 950–954.

National Academy of Sciences (2016), *Next Generation Earth System Prediction: Strategies for Subseasonal to Seasonal Forecasts*, National Research Council, National Academy of Sciences, Washington DC ISBN-978-0-309-38880-1, 290 pages.

Neena, J. M., J. Y. Lee, D. Waliser, B. Wang, and X. Jiang (2014), Predictability of the Madden–Julian Oscillation in the Intraseasonal Variability Hindcast Experiment (ISVHE), *J. Climate*, *27*, 4531–4543, doi:10.1175/JCLI-D-13-00624.1.

Petch, J., D. Waliser, X. Jiang, P. Xavier, and S. Woolnough (2011), A global model inter-comparison of the physical processes associated with the MJO *GEWEX News*, August.

Peters, M., and C. Bretherton (2006), Structure of tropical variability from a vertical mode perspective, *Theor. Comput. Fluid Dyn.*, *20*, 501–524, doi:10.1007/s00162-006-0034-x.

Peters, O., and J. D. Neelin (2006), Critical phenomena in atmospheric precipitation, *Nat. Phys.*, *2*, 393–396.

Pritchard, M. S., and C. S. Bretherton (2014), Causal evidence that rotational moisture advection is critical to the superparameterized Madden–Julian Oscillation, *J. Atmos. Sci.*, *71*, 800–815, doi:10.1175/JAS-D-13-0119.1.

Raymond, D. J. (2001), A new model of the Madden-Julian Oscillation, *J. Atmos. Sci.*, *58*, 2807–2819.

Raymond, D. J., S. L. Sessions, and Z. Fuchs (2007), A theory for the spinup of tropical depressions, *Quart. J. Roy. Meteor. Soc.*, *133*, 1743–1754, doi:10.1002/Qj.125.

Raymond, D. J., S. Sessions, A. Sobel, and Z. Fuchs (2009), The mechanics of gross moist stability, *J. Adv. Model. Earth Syst.*, *1*, 20, doi:10.3894/james.2009.1.9.

Sobel, A., and E. Maloney (2012), An idealized semi-empirical framework for modeling the Madden–Julian Oscillation, *J. Atmos. Sci.*, *69*, 1691–1705, doi:10.1175/jas-d-11-0118.1.

Sobel, A., and E. Maloney (2013), Moisture modes and the eastward propagation of the MJO, *J. Atmos. Sci.*, *70*, 187–192, doi:10.1175/Jas-D-12-0189.1.

Sobel, A. H., J. Nilsson, and L. M. Polvani (2001), The weak temperature gradient approximation and balanced tropical moisture waves, *J. Atmos. Sci.*, *58*, 3650–3665.

Sobel, A. H., E. D. Maloney, G. Bellon, and D. M. Frierson (2008), The role of surface heat fluxes in tropical intraseasonal oscillations, *Nat. Geosci.*, *1*, 653–657, doi:10.1038/Ngeo312.

Vitart, F., et al. (2012), Subseasonal to seasonal prediction: Research implementation plan, WWRP/THORPEX-WCRP Report.

Waliser, D. E. (2012), in *Predictability and Forecasting, in Intraseasonal Variability in the Atmosphere-Ocean Climate System*, edited by W. K. M. Lau and D. E. Waliser, Springer, Heidelberg, Germany.

Yu, J. Y., and J. D. Neelin (1994), Modes of tropical variability under convective adjustment and the Madden-Julian Oscillation. 2. Numerical results, *J. Atmos. Sci.*, *51*, 1895–1914.

Zhang, C. (2013), Madden–Julian Oscillation: Bridging weather and climate, *Bull. Am. Meteorol. Soc.*, *94*, 1849–1870, doi:10.1175/bams-d-12-00026.1.

Zhang, C., J. Gottschalck, E. D. Maloney, M. W. Moncrieff, F. Vitart, D. E. Waliser, B. Wang, and M. C. Wheeler (2013), Cracking the MJO nut, *Geophys. Res. Lett.*, *40*, 1223–1230, doi:10.1002/grl.50244.

Zhang, G. J., and N. A. Mcfarlane (1995), Sensitivity of climate simulations to the parameterization of cumulus convection in the Canadian Climate Centre general circulation model, *Atmosphere-Ocean*, *33*, 407–446.

Zhao, M. (2014), An investigation of the connections among convection, clouds, and climate sensitivity in a global climate model, *J. Climate*, *27*, 1845–1862, doi:10.1175/JCLI-D-13-00145.1.

Zhao, M., et al. (2016), Uncertainty in model climate sensitivity traced to representations of cumulus precipitation microphysics, *J. Climate*, *29*, 543–560, doi:10.1175/JCLI-D-15-0191.1.